Nanotechnology Perceptions
ISSN 1660-6795
www.nano-ntp.com

Scanning Tunneling Microscopy: A Review

José Ricardo Macías Barberán[1]

1Universidad Técnica de Manabí. acultad de Ingeniería Agronómica, Carrera de Ingeniería Ambiental, Grupo de Investigación Agricultura Sostenible y Bioenergía, Facultad de Ciencias Básicas, Departamento de Física, Facultad de Agrociencias Departamento de Procesos.
jose.macias@utm.edu.ec . ORCID: https://orcid.org/0000-0002-2857-6867

The study of surfaces and manipulation of materials of nanometric size is a method widely used in different areas of research. The scanning tunneling microscope (STM) is a valuable instrument that allows working on these two aspects with elements of scientific interest. This article tries to explain the principles and applications of the STM based on attractions and repulsions of atoms at very small distances to collect information, which once processed and analyzed is converted into images visible to the human eye. The review was carried out through the search and analytical reading of scientific papers and publications such as Google Scholar, Scopus, Scielo, Redalyc and Doaj. The contextualization of quantum tunneling was established focused on the importance, applicability and development of the STM which has allowed the new advances developed throughout the 21st century.

Keywords: tunneling, quantum mechanics, nanotechnology

1. Introduction

For many years, at the center of quantum mechanics was the idea that matter behaved like a wave and like a movie. From the nineteenth century onwards, experimentally it was shown that by looking more closely at the behavior of very small elements, such as molecules, atoms, and particles, intuitive classical predictions had not been adequate to predict the results of experiments.

The fundamental reason for this conception was that all these elements were treated as point objects whose position and momentum could be predicted with absolute certainty. However, from the twentieth century onwards, the idea began to take shape that these tiny materials can behave like waves at certain times and like particles at others, managing to accurately predict their behaviour (Oyvind, 2020).

In this sense, one of the most interesting discoveries of quantum mechanics is that due to the natural wave shape of matter, small particles can be found in places that would be impossible from the classical point of view (Vitti *et al.*, 2020). This phenomenon is called quantum tunneling, and it has allowed new advances that have been developed throughout the 21st century. Among those applications are: scanning tunneling microscope, tunneling diodes, tunneling field effect transistors and the compression of radioactive decay (drives any nuclear power plant), therefore they play a fundamental role in society.

Later it became impossible to see the fundamental blocks of matter, perceiving an atom was only possible under the theoretical conception of these, but thanks to electron microscopes, it is now possible to see and even form figures of the size of an atom thick (Suzuk *et al.*, 2020). The importance of these advances is only being developed with nanotechnology, which in the future will allow us to see everything that happens in matter around us. The study of surfaces and manipulation of nano-sized materials is a method highly used in different areas of research. The Scanning Tunneling Microscope (STM) is a valuable instrument that allows us to work on these two aspects, since through it, the characterization of surfaces and experimentation with elements of scientific interest can be achieved (Peña, 2020).

The study and development of new technology is one of the main applications of electron microscopes, in this article Scanning Tunneling Microscopy is presented supported by the tunneling effect as a basic principle of operation, which uses the attractions and repulsions caused by atoms at very small distances to collect information, which after being processed and analyzed, is converted into images that can be seen with the naked eye.

2. Methodology

The methodological foundation for this research was documentary, based on methodical reasoning to establish the constructs, generating truthful and accurate information comparable to other updated scientific sources. The review was developed in the following phases:

Preparatory or initiation: The dissemination of tunneling was selected as the central theme, conducting research in March 2023 in indexed databases for scientific articles.

Exploration: Google Scholar, Scopus, Scielo, Redalyc, Doaj, among other online sources, were used for documentary search.

Formulation: Establishment of the documentary references for the study period, reaching the contextualization of the topic focused on the importance, application and development of the STM for scientific studies.

Collection: included the compilation, classification and recording of the information extracted from the reviewed documents. To this end, manual categorization was used using Mendeley software, establishing subcategories.

Selection: the selected material was organized in tables, presented with common characteristics of the documents such as author, year of publication, title, description of the work according to the classification emphasis and the purpose of the study.
Interpretation: From the background analysis, common aspects and distances between the articles were identified to make comparisons that allowed the construction of the arguments of the emerging scientific trends.
Theoretical construction: drafting of the final document to make it known in the national and international scientific community.

3. Results and Discussion

Tunneling Basics

Generally speaking, tunneling consists of probing energetically forbidden areas by particles, allowing various applications in a wide range of systems. It was proposed by Gamow in 1928 as the mechanism behind the mysterious α radiation. The spin tunneling effect consists of the transition of the magnetic states of a molecule through classically forbidden states (Gil *et al.*, 2022).

Quantum tunneling plays a key role in a plethora of phenomena beyond condensed matter physics and is applied to many different systems, including MOSFETs, resonant tunneling diodes (RTDs), electrical conduction in quantum dots, superconductivity, scanning tunneling microscopy, reaction kinetics, and biological processes (Martín-Palma, 2020).

Moreover, tunneling makes possible significant complexity in molecular and biological evolution by providing different sources of constant energy flux over a long period of time, enabling synthesis pathways for astrochemical reactions that would not otherwise occur, and influencing specific functions of biomolecular nanomachines that sustain the process of life (Vuković, 2021). These processes include chemical evolution within the cold interstellar medium and within stars, prebiotic chemistry in the subsurface and atmosphere of planetary bodies, the increase and persistence of habitable conditions through insolation and geothermal heat, and the function of complex biomolecules (Trixler, 2021).

Tunneling is a non-trivial quantum phenomenon that becomes effective at scales of around one nanometer and below. It allows elementary particles and atoms to overcome an energy barrier without having enough energy to overcome it. That seemingly paradoxical phenomenon might seem like an exotic process that is only important for particle physics and quantum physics applications, such as the tunneling diode or scanning tunneling microscopy (Gil *et al.*, 2022). The delay time of a quantum tunneling particle is independent of the thickness of the opaque barrier, this is called the Hartman effect and can result in particles traveling faster than light (Oyvind, 2020).

The scanning probe microscope is a fundamental tool in nanoscience and nanotechnology, capable of providing resolution up to the atomic scale in real space. Its basic principle of operation consists of moving a very fine tip close to a surface, so that several properties can be measured with manometric or atomic resolution (Martínez, 2022). The STM was developed in 1981/1982 by researchers Heinrich Rohrer (Swiss) and Gerd Binnig (German) at IBM's laboratories in Zurich, winning the Nobel Prize in physics in 1986.

The STM operating principle is based on a quantum effect known as tunneling. In this case, the electrons, thanks to their dual nature between wave and particle, have the probability of crossing a potential

barrier with energy greater than their kinetic energy (Peña, 2020). Tunneling is a purely quantum-mechanical process by which a microscopic particle can penetrate a potential barrier even when its energy is less than the height of the barrier. In classical mechanics, a particle with energy ***E***, upon encountering a potential barrier ***V0*** in its path, will be reflected in it if ***V0*** > ***E*** (Mamedaliev, 2018).

The potential barrier is illustrated in Figure 1. When the height **U0** of the barrier is infinite, the wave packet representing an incident quantum particle is unable to penetrate it, and the quantum particle bounces off the barrier boundary, just like a classical particle. Likewise, if the width *L* of the barrier is infinite and its height is finite, a part of the wave group representing an incident quantum particle may leak across the barrier boundary and eventually perish after traveling a certain distance within the barrier (Moebs *et al.*, 2021).

Thus, in region **I**, where **X < 0**, an incident wave group (incident particle) moves in a potential-free zone and coexists with a reflected wave group (reflected particle). In region **II,** a part of the incident wave that has not been reflected in **X = 0,** moves as a transmitted wave in a constant potential U**(x) = +U0** and passes through tunnels through region **III** in **X = L**. In region **III** for **X > L**, a group of waves (transmitted particle) that has crossed the potential barrier moves as a free particle in the potential-free zone. The horizontal line indicates the energy ***E*** of the incident particle (Moebs *et al.,* 2021).

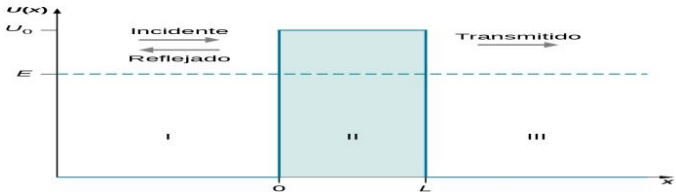

Figure 1. Illustration of a potential energy barrier of height U0 creating three physical regions with three different wave behaviors. Taken from: Moebs *et al.,* (2021). In original language Spanish

Similarly, when a uniform, time-independent beam of electrons or other quantum particles with E-energy traveling along the x-axis (in the positive right direction) encounters a potential barrier. The question is: What is the probability that an individual particle in the beam will pass through a tunnel through the potential barrier? The answer can be found by solving the boundary condition problem for the time-independent Schr ödinger equation for a particle in the beam (Moebs et al., 2021). Threetypes of solutions to the stationary Schrequation ödinger have been proposed for the quantum tunneling problem. An oscillatory behavior in regions **I and III**, where a quantum particle moves freely, and another exponential decay behavior in region II (the barrier region), where the particle moves in the **potential U0**. (Figure 2).

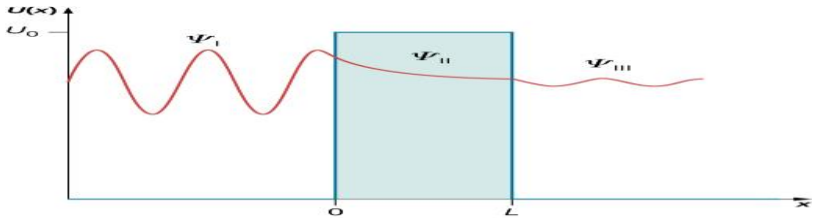

Figure 2. Illustration of the solutions to the Schrö dinger stationary equation for the quantum tunneling problem. Taken from Moebs *et al.,* (2021).

On the other hand, this technique allows not only the topography of the surface of a material, but also offers the possibility of studying molecules and atoms, such as the manipulation of individual molecules on metal surfaces, the surface modification of the material at the atomic scale and the measurement of the variation of the electronic properties on its surface. The latter is a technique known as tunneling spectroscopy that allows the electronic structure of the sample to be obtained, making use of differential conductance. This tunneling microscopy technique has the ability to be developed in various media, particularly effective in ultra-high vacuum (UHV), or controlled atmospheric environments, since the current signals generated are in the order of nano to peak amperes, very sensitive to changes in the environment (Oyvind, 2020).

Advantages and Disadvantages of STM

According to Martín-Palma (2020), among the advantages, the ease with which the symmetry that a material under study should have can be obtained (which would allow us to exclude many of the structures that should be verified for the study of X-rays; since, after all, the results of both experiments must match). In addition, there is the possibility of finding the shape of the density of material states at each point, given the nature of the tunnel strength formula. Among the disadvantages, this author points out that STM only refers to conductors and semiconductors, due to the reason for their operation. Moreover, it is extremely sensitive to noise and must be subjected to high vacuum to make the measurement more accurate.

According to Oyvind (2020), compared to the atomic force microscope AFM, the STM method is obsolete, as the former allows measurements of the structure for all types of materials (regardless of their conductive nature). However, the STM is advantageous in terms of the possibility of measuring the density of states; and, it should be said, that it cannot generate disturbances on the surface of the material because it is not in contact with it (unlike AFM).

Bardeen model for tunneling

An atomic-scale topographic image can be defined as an image of the constant surface charge density. Nonetheless, the STM tip follows the local density of Fermi-level states, while all electrons contribute to charge density (Oyvind, 2020).

Physicist John Bardeen, Nobel Laureates in Physics for the transistor and BCS theory for superconductivity, developed a model for tunneling in solids considering this effect at metal-insulator-metal junctions. Their approach was to consider the tip plus the barrier and the sample plus the barrier, as two separate systems. The electronic states of the two subsystems can be obtained by solving the time-independent Schrondinger equation. For the simplified one-dimensional case, the solutions are oscillatory wave functions with exponential decay within the barrier. However, for the three-dimensional case, the solutions are the complete wave functions of the tip and the sample, taking into account the atomic arrangement (Martínez, 2022).

Measurement Modes in STM

There are basically 2 modes for imaging the surface of the sample under study, which are related to the height of the tip to the sample and to the dependence of the tunnel current on it; therefore, a current

flow that is proportional to the sum of the probabilities that an n number of electrons between an $EF-eV$ energy can cross the vacuum barrier according to the equation of Schrondinger:

$$I \sim \Sigma_{EF-eV}^{EF} |\psi n(0)|^2 e^{-2k11x}$$

Where x is the distance between tip y shows in this case d. Local state density (LDOS) which describes the number of accessible electronic states of a system per unit volume, close to the Fermi level at a defined energy $EF-eV$ (Oyvind, 2020).

The topography image will be a constant and the current image is given by the changes in the tunnel current associated with the variation in the relative distance between the tip and the sample, produced by the corrugation of the surface (Figure 3).

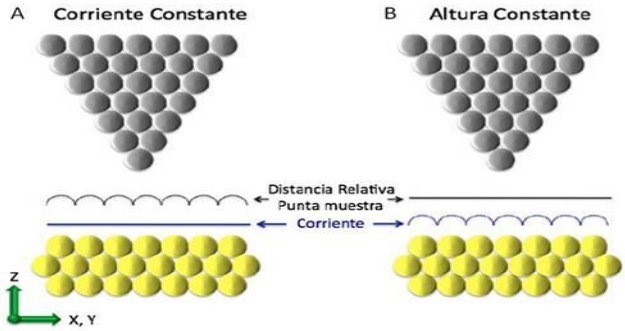

Figure 3. Measurement modes in STM. Taken from Delgado *et al.*, (2019). In original language Spanish

Constant tunnel current mode

It consists of moving the tip on the surface, adjusting the vertical distance between them by means of the piezo **z**, the tunnel current is kept constant by adjusting the height of the tip to the sample by means of a feedback circuit that applies a voltage to the piezotube on the z-axis, these variations of z are recorded, while the sweep is carried out (Delgado, *et al.,* 2019).

According to Sainadh et al., (2019) the variations in z correspond to the variations in the height of the surface of the sample that will be interpreted as surface irregularities, generating with these data a resulting image of the surface called a topographic image.

In this same context, according to Martínez (2022), the local state density (LDOS) of the sample for the Fermi level (absolute square of the wave function for the Fermi energy) shows an oscillatory behavior along the **X** coordinate (parallel to the surface) on the surface (**z=0**).

Constant Height Mode

In this case, the feedback circuit is turned off, a constant height is set from the tip to the sample while the sweep is carried out and the variations of the tunnel current are recorded as it passes (Delgado, *et al.,* 2019). There are several problems with implementing this mode, as maintaining constant height during scanning on an atomically flat terrace is complicated by the effects of thermal drift and piezoelectric influence. In addition, when scanning on an edge of an atomic passage, the tip-sample distance changes in several Angstroms, causing a significant alteration in the tunnel current (Martínez,

2022), which is why it is recommended to use it for work at low temperatures as this will provide atomically flat surfaces.

Tunneling spectroscopy (STS)

There is another mode of measurement known as Scanning Tunneling Spectroscopy; STS), which allows us to know the electronic structure of the sample, in itself to know the LDOS of the sample. To study it, differential conductance is used, defined as the derivative of the tunnel current with respect to the bias voltage (Bohórquez, 2017).

Tunneling time

The problem with tunneling time is the fact that a semiclassical estimate of a particle's velocity becomes imaginary since its kinetic energy within the barrier is negative. Therefore, making obvious the approximation that the duration of a tunnel event is the width of the barrier divided by velocity produces non-physical results (Field, 2022). In this regard, sophisticated approaches have been devised, but apparently have not found a satisfactory solution; although recently, experimental techniques have been developed that allow events in the attosecond range to be measured (Martín-Palma, 2020). A recent study has set an upper limit of 1.8 attoseconds as in any tunneling delay (Sainadh *et al.,* 2019).

However, although most experimental results seem to indicate that quantum tunneling is not an instantaneous process, there is no general consensus from a theoretical point of view (Hofmann *et al.,* 2019). A finite time delay (Hartman effect) has been evidenced, although the delay time for a quantum tunneling particle is independent of the thickness of the potential barrier above a given value (Martín-Palma, 2020). This delay is shorter than the "equal" time, i.e., the time it would take for a particle of equal energy to travel the same distance L in the absence of the barrier (Petersen and Pollak, 2017).

According to (Petersen and Pollak, 2018) tunneling time cancels out and is independent, not only of the width but also of the height of the barrier for a square and a symmetrical or asymmetric Eckart barrier potential, thus generalizing the Hartman effect to time-independent one-dimensional potentials. In addition, they also showed that for a square barrier, in a vanishing tunnel time does not lead to the experimental measurement of velocities greater than 1.8 attseconds.

Tunneling Time in the Broglie-Bohm Theory

From the point of view of quantum mechanics, each tunneling particle travels through the barrier in a state intended to be transmitted, or in a state that is destined to end up reflected (Broglie-Bohm theory). Whereas in the orthodox interpretation, a tunneling particle interacts with the barrier in a state of superposition that cannot be divided into eventually transmitted and occasionally reflected components (Field, 2022).

The uncertainty principle prevents us from having a clear notion of reality, by observing the behavior of a particle in the barrier region, and seeing which of these trajectories it is following because there is only access to the behavior of the wave function, which allows both transmitted and reflected trajectories. Following the de Broglie-Bohm theory, analogously each particle that impinges on a double slit passes through the left slit or the right slit in a localized deterministic trajectory (Suzuk *et al.,* 2020). The same doubt occurs when tracking the behavior of a particle in a double slit and specifying which slit it is passing through, since only the behavior of the wave function is known, which allows both left and right slit trajectories (Field, 2022).

Study surfaces at STM

Graphite

Graphite is used because it is quite easy to get good images of its atomic structure, because it has a flat and inert surface. In particular, highly oriented pyrolytic graphite (HOPG) has been used. HOPG has a high degree of crystallographic orientation, tending to prefer C-axes perpendicular to the substrate (Dakhlaoui *et al.,* 2021).

The graphite atoms are arranged in a hexagonal fashion, forming a network similar to a honeycomb (Figure 4). In the upper layer the black atoms are located just above an atom of the lower layer, while the orange atoms projected on the same plane are located in the center of the lower hexagon, therefore, the electrical conductivity of the surface varies locally, as does the signal received by the STM. perceiving orange atoms as taller (Sanahuja, 2015).
Delgado *et al.* (2019), used HOPG.

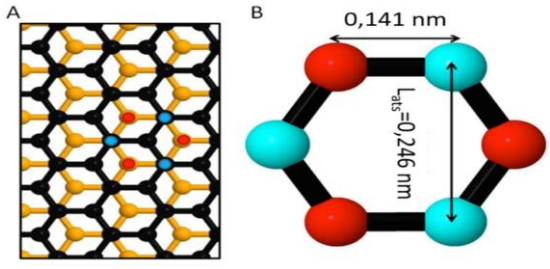

Figure 4. Arrangement of HOPG atoms. Taken from: Sanahuja, (2015).

Gold (Au)

Gold features atomic-sized terraces and steps. It has been reported that a step whose height is a single atom measures 0.20 0.02 nm, therefore knowing these values can calibrate the distance in the STM (Rubio *et al.,* 2017). In this sense, Delgado *et al.* (2019), used gold oriented in the crystallographic direction (111)

Graphene

This material has become important because it is the first two-dimensional material found and because of the multiple properties it presents, hence its applications are also numerous in electronics, energy and biotechnology among others; in addition, fexOy graphene hybrid materials are synthesized quite quickly, they have magnetic properties such as super paramagnetism and ferrimagnetism (Sanahuja, 2015). The arrangement of the graphene atoms can be visualized in Figure 5.

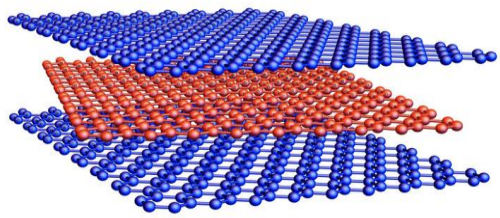

Figure 5. Arrangement of graphene atoms. Taken from: Dakhlaoui *et al.,* (2021).

Other surfaces

In this case, Martin and Vélez (2018) experimented with a classical anti-ferromagnetic chain of iron (***Fe***) atoms deposited on a thin, insulating substrate. When they scanned the sample with a nonmagnetic tip, each Fe atom looked identical. However, when scanning with a magnetic tip, they observed that 4 of the Fe atoms protruded from the topography while the other 4 appeared to be at a lower altitude.

This could have occurred because of a change in the tunnel current that occurred when the tip, with a polarized spin magnetic atom, encountered opposite alignments of Fe's atomic spins as it traveled along the chain. The authors attributed this difference to magnetoresistance at the atomic scale. Depending on whether the atomic spin is positioned parallel or anti-parallel to the magnetic field of the tip, the amount of current flowing through the STM also varies. This chain is assumed to be in a classical magnetic state called the Néel state, in which the orientations of the consecutive spins are opposite (Bohórquez, 2017).

In other experiments, ZnO films of two natures have been used, a single crystal with a polished Zn face and orientation (0001), and the second of films grown by the atomic layer deposition method (Bohorquez, 2017). The surface of silicon (Si) oriented in the direction (111) has also been studied under ultra-high vacuum conditions, at a pressure of 10/10 Torr (Serkovic, 2009).

Likewise, Goldman *et al.* (2022), proposed a model to determine diffusion rates in H/PuO2 (plutonium oxide) systems, establishing it as a rapid detection tool to assess potential quantum damage and nuclear vibration effects on any number of condensed-phase materials and surfaces, where hydrogen tends to follow well-defined minimum energy paths.

On the other hand, Zhu *et al.,* (2022) analyzed the transfer of hydrogen atoms (HAT) during the degradation of poly-a-methylstyrene (PAMS), which is usually attributed to the thermal effect, but unexpectedly exhibited a strong tunneling effect at high temperature, although the energy barrier of the HAT reaction is only 10 of a magnitude different from depolymerization, The probability of tunneling of the former may be 14 to 32 orders of magnitude higher than that of the latter. The work highlights that quantum tunneling may be a major source of uncertainty in the degradation of PAMS, which will provide a direction for the further development of key target fabrication technology in inertial confinement fusion (ICF) research and even the solution of plastic pollution.

Dissipation in tunneling

Atomic resolution and stable spectroscopy can be obtained only if the system is well isolated from external mechanical vibrations. To achieve high resolutions, it is essential to minimise all the sources of noise that can affect this type of system, which are mainly mechanical vibrations and electrical noise. After many experiments, the vacuum has been used as a dielectric medium, precisely due to the vibrations that affected the tunnel separation (Martín & Velez, 2018).

Another major problem in the frequency spectrum that can affect STM is the intrinsic resonance frequencies of the experimental system. The vibratory effect of the system will be the amplification of the external disturbance, which will be to the clear detriment of the resolution. A compact and rigid STM design has been shown to minimize these problems by shifting the system's own frequencies to high

frequencies (~kHz) (Moreno, 2015). These disturbances can be the limiting factor of resolution and even cause erratic movements of the scanner, as well as lead to incorrect readings of certain experimental parameters such as the temperature inside the scanner (Klimenko, 2021). Some alternatives can be implemented to solve these situations:

First, a well-defined and clean electrical ground must be placed on the entire STM. This soil is common to the entire system, including electronics, computers, and metal shelves. In this regard, Moreno (2015) used a star-type configuration to avoid ground loops, characterized by a copper (Cu) metal plate where several flat copper braids are welded together that give ground to other points.

A second alternative is that the STM heads are manufactured as small and light as possible to increase their mechanical resonance frequency. The heads are isolated from the environment by means of pass filters under the elastic table (Klapetek and Anderson, 2022). In this case, Vitti *et al.* (2020) used titanium and ceramic heads.

Third, the STM's wiring must also be shielded throughout its path and in contact with the system's ground. This is essential to avoid problems of mutual electromagnetic induction or high-frequency (RF) antenna effect from the outside (Vitti *et al.,* 2020).

Finally, another form of insulation consists of pneumatic anti-vibration dampers, powered by compressed air. The use of 3 or 4 dampers support the entire system including the STM, cameras, pumps and a part of the electronics that allows the microscope to be effectively isolated from mechanical disturbances of the environment Klimenko, (2021).

Symmetries and tunneling

Symmetry has to do with the effect of the application of operators on a system and depending on the response obtained, it is determined whether or not there is a symmetry, when a change in the system occurs or not (Petersen & Pollok, 2018). A problem that compensates for this symmetry is the symmetrical double well, which corresponds to an elementary case but very instructive to understand this symmetry (Figure 6).

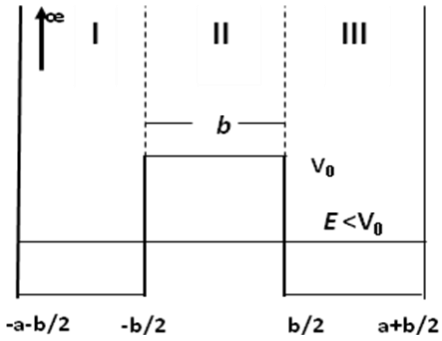

Figure 6. Symmetrical double well. Taken from Juárez and Fernández (2018).

Two potentials: Double well of finite potential

According to Juárez and Fernández (2018), when a change in the system occurs, Schrödinger's stationary equation for regions I and III is:

$$\frac{-h2\ d^2}{} \psi(x) = E\psi(x) \Rightarrow d2\ \psi(x) = -k2\psi(x)$$

$2\mu\ dx2\ dx^2$

with k2 = (2μ/h2)E, so the solutions in these regions are given by:

Region I (−l < x < −b/2)

ψI (x) = Asen(k(x + l)),

Region III (b/2 < x < l)

ψIII(x) = Dsen(k(x − l)),

where l = a + (b/2).

For region II (−b/2 < x < b/2) the Schrödinger equation is given as follows:

$$\frac{-h2\ d^2}{2\mu\ dx2}\ \psi(x) + V0\ (x)\ \psi(x) = E\psi(x)$$

$$\Rightarrow \frac{d2}{dx2}\ \psi(x) = q2\ \psi(x)$$

where, q2 = (−2μ/h2)(E – V0 (x)) with q > 0 since E < V0(x) and the solution for this region is:

ψII (x) = B exp(qx) + C exp(−qx)

There are 2 alternative solutions to solve this situation: the symmetrical solution and the antisymmetric solution. In addition, these alternatives will be determined by the relationships between the coefficients, respecting the continuity of the wave function and its derivatives (Juárez and Fernández, 2018).

Symmetrical solution (Figure 7)

$\Psi s(-x) = \psi_s(x) \Leftrightarrow As = -D_s \& Bs = Cs$

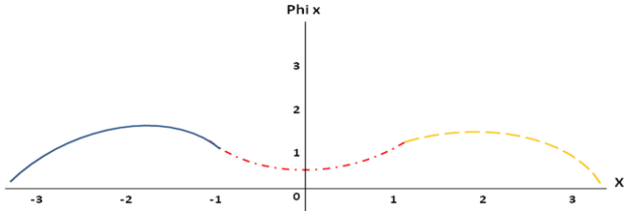

Figure 7. Graphical representation of symmetrical states. Blue Line: Region I; Red line: region II; Orange Line: Region III. Taken from: Juárez and Fernández (2018).

Antisymmetric solution (Figure 8)

$\Psi a\ (-x) = -\psi_a(x) \Leftrightarrow Aa = D_a$ and $Ba = -Ca$,

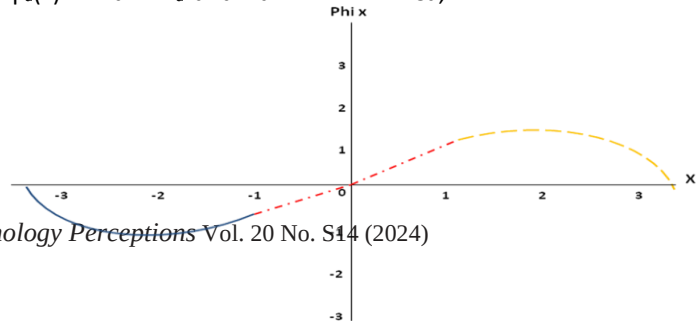

Figure 8. Graphical representation of antisymmetric states. Blue Line: Region I; Red line: region II; Orange Line: Region III. Taken from: Juárez and Fernández (2018).

In the same order, in Figure 9 it can be seen that the energies associated with the symmetrical and antisymmetric states approach each other as the depth of the well grows, that is, degeneration appears for very large potentials (without considering the limit case at infinity, because if this occurs, the wells become independent) (Juárez and Fernández, 2018).

Figure 9. Comparison of energy-determining functions for antisymmetric symmetric states. Blue line: ***f* (q)** = (1/q) cot h(q/2); Red line: ***f* (q)** = (1/q) tan h(q/2). Taken from: Juárez and Fernández (2018).

It can be noted that when symmetrical and anti-symmetric states are superimposed, the symmetry is broken, which could be contradictory; however, as has been shown in the development of the right and left states, it is thanks to the formation of these states that the correct description of phenomena commonly observed in nature can be given (Petersen and Pollok, 2018). Symmetry and its breaking, and the tunneling effect, are tools that allow an explanation to be given to those small details, which are present in the environment on a daily basis and are rarely discussed as they are given as true (Prastowo *et al.,* 2020).

Experimental STM Configuration

The STM has an atomically sharpened conductive tip (extremely fine) located at a distance of the order of Ängstrom (Ä) from the surface of the sample, operated in a controlled manner on the surface, thanks to the use of piezoelectric devices and control electronics that allow scanning in the three directions **X, Y** and **Z (**McDonald et al., 2019).

When a potential difference is applied between the tip and the sample (bias voltage) the electrons from the tip cross the potential barrier (quantum tunneling) and reach the sample or vice versa, establishing a tunnel current. This tunneling electron current is continuously monitored while the tip is in motion, so the amount of current at the location (x,y) gives information about the elevation of the tip above the surface at this location (Figure 10). By recording variations in such current during scanning, a topographic image of the surface can be reproduced at atomic resolution and displayed on the computer monitor (Moebs *et al.,* 2021).

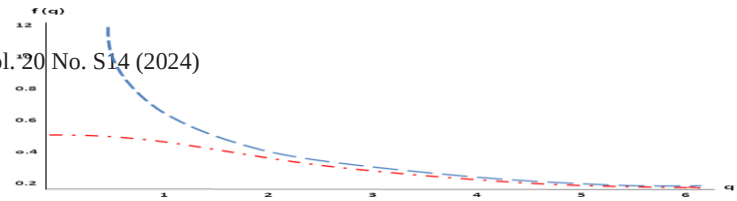

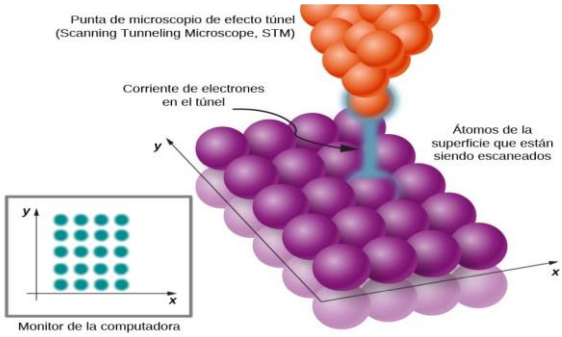

Figure 10. Illustration of the scan with a narrow tip along the surface with a constant potential. Taken from Moebs et al. (2021). In original language Spanish

In this same context, Figure 11 illustrates a diagram of the experimental configuration of the STM, where the tip with the thickness of an atom is observed that performs a sweep on the surface of the material detecting a tunnel current that is amplified, then filtered by the Lock-In and finally these variations generate the topographic image.

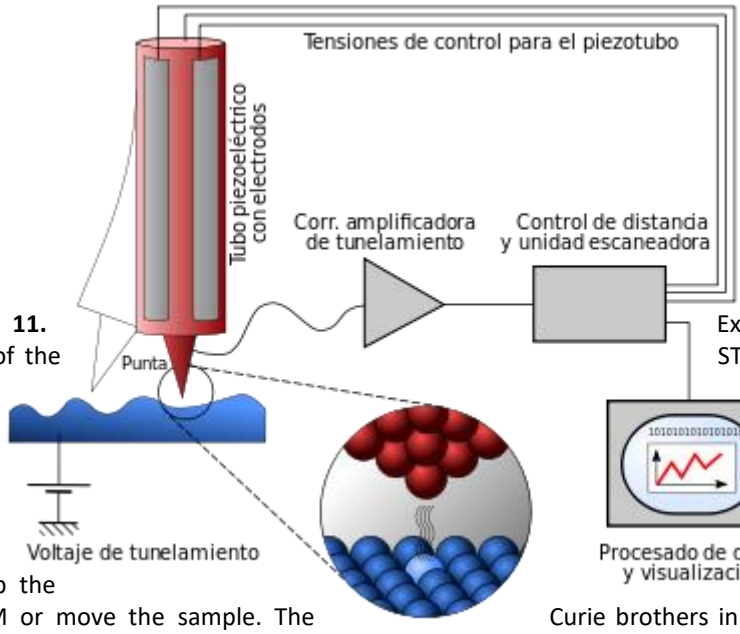

Figure 11. Experimental configuration of the STM. Taken from: Moebs *et al.* (2021). In original language Spanish

Pizoelectric Effect

Piezoelectric actuators are used to sweep the surface with the tip of the STM or move the sample. The Curie brothers in 1880 discovered the piezoelectric effect; this occurs when certain materials are subjected to a mechanical stress that gives rise to an electrical polarization, thus appearing a potential difference (Bohórquez, 2017). The opposite effect can also occur, when applying a voltage to the electrodes that induces an electric field, causing the expansion of the piezoelectric material, and this is because the unit cell is deformed by the applied electric field (Martínez, 2022).

The deformation of piezoelectric materials depends on the internal electrical polarization, these deformations can be shear-type or normal. The first occurs when the voltage is applied perpendicular to the internal electrical polarization of the material; in normal deformation, the electrical polarization is parallel to the applied voltage, resulting in elongation with linear contraction of the material (Delgado *et al.,* 2019).

Tip Preparation

To achieve the correct operation of the STM and obtain good quality images of the surfaces, the preparation of the scan tip is essential. This tip must have a sufficiently narrow diameter to be able to reach all possible wells on the surface to be scanned (Martínez, 2022), but it must also be as sharp as possible so that a single atom remains at the end (Delgado, *et al.,* 2019).

In ambient conditions, it is common for tips to be made from materials that do not rust easily when in contact with air, such as platinum or iridium. But these types of tips will only work on very flat surfaces such as graphite (Klapetek & Anderson, 2022).

In the case of gold, tungsten tips prepared with the sputering technique have been used, dipping the tip in KOH, the non-immersed side is attached to a cathode/anode. The electrolysis process dissolves the tip by separating all the surface irregularities where the current is concentrated (Paganini & Pérez, 2011).

Feedback Control

Generally, in order to describe the topography of the surfaces, STMs have a feedback system. Normally, in these systems you have a loop that constantly measures the output of system **X** and compares it with the fixed point **W** where you want to work, subtracting both **W-X**. This gives an error signal that is introduced into the system to get the exit point to adjust to the fixed point **W** taking into account external noise (Martínez, 2022).

In this regard, Avila and Gualteros (2016), designed a controller by the LGR method, initially obtained a good response but as the acquired tunnel current has a lower order of magnitude, the controller tends to be unstable. On the other hand, the adaptive controller designed through SIMULINK in MATLAB® for tunnel currents of small magnitude the system continues to be stable, although it becomes slower; Therefore, in the choice of controller, a little speed is sacrificed for stability.

In gold, the process is powered and regulated by a controller that has a maximum voltage of 20v, and ends when the circuit has a current lower than this (Paganini & Pérez, 2011). Likewise, Martínez et al. (2016), for the interface between the computer and the microscope, implemented an OMB-DaqBoard/2000 data acquisition card.

Image Processing

The data obtained by scanning probe microscopes, such as the STM, are in the form of a matrix, where the topography (height of the tip above the surface), or other magnitudes such as the tunnel current, are measured according to the lateral **XY** position of the surface to be studied (Banerjee and Zhanga, 2019). Corresponding gray levels can be assigned to these measured heights for an optimal image. In addition, image processing is employed to further improve the representation of such images, for example, by removing high-frequency noise, noise pixels, or noise lines (Martínez, 2022).

In this regard, Delgado *et al.* (2019) processed the STM images in HOPG and gold samples using the constant current method, where bias voltage of 100 mV and an amplification of 109 were used.

Sample scanning with STM

Once the STM electronics are turned on, you must start with a rough approximation of the tip towards the sample to be analyzed. The bias and the tunnel current that is desired must be fixed. It should be considered that if the bias is decreased, the tip is approached, and if the tunnel current is decreased, the tip moves away (Banerjee & Zhanga, 2019).

The auto-approach function allows the tip to be brought closer to the sample automatically. This process takes place in different steps, in each step the tip is brought closer to the sample and the tunnel current is verified. If the work point that is being requested has not yet been detected, the next step is taken. At each step, you can see how the piezoelectric actuators extend and contract to approximate and retract the tip (Klapetek & Anderson, 2022).

According to (Vitti *et al.,* 2020), once the optimal distance to the sample is achieved, the appropriate parameters are determined to initiate an extensive sample scan. The initial sweep is performed at constant current in an area of approximately 400 nm on a side, the P-gain is set to 12, the I-gain to 13, time-line 0.25 sec and the current is set to 1 nÄ. Subsequently, a region that presents few variations in height and that these are relatively mild (to avoid peaks or wells that produce collisions with the tip) is sought. Progressively, regions with a more precise measurement in a highly flat area are delimited; the parameters are changed from constant current to constant height, P-gain and I-gain go to approximately 2, time-line is set to 0.06 sec and the current set point is increased to 2 nA.

When the working point has been reached, it is advisable that the tip is not fully extended or retracted, so that when the scan is carried out it can be moved without reaching the limit. Then, by fine-tuning it is possible to leave the tip in an intermediate position (Klapetek & Anderson, 2022). In this regard, Moebs *et al.* (2021) have presented an image of approximately 5 nanometers for a surface sample of copper, where copper atoms are contained within a quantum enclosure of 48 iron atoms. The circular iron barrier has a radius of 71.3 Angstroms (71.3 x10-10) meters, and electrons are observed to behave like waves (Figure 12).

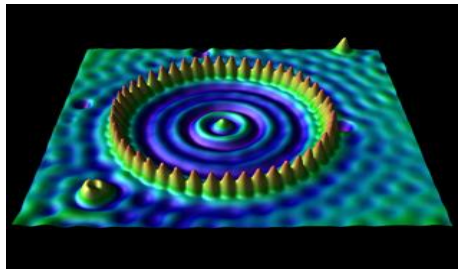

Figure 12. Image taken with a scanning tunneling microscope. Taken from: Moebs *et al.* (2021).

In the same order, Martínez *et al.* (2016), developed a program in LabVIEW that generates the signals required for X-Y scanning, and simultaneously acquires the Z voltages related to the tunnel current between the tip and the sample. The program builds the microscopy image of the studied surface from the Z voltages.

For their part, Delgado *et al.* (2019), showed different terraces and steps corresponding to the crystallographic direction (111) of the Au. Below the topography image, they placed the scale of colors used and its equivalent range in nanometers. They also observed the atomic steps and the terraces of HOPG, placing at the bottom of the figure the color scale corresponding to the height of the steps on the **Z** axis, and a gray line that represents the area where the topographic profile of the steps has been analyzed.

Image processing with STM

After working with the STM, "raw" images are obtained that often have to go through a manipulation process to improve their quality as well as to analyze them and obtain more accurate information than what is recorded in the image. In order to improve the quality of images, there are various computer programs that allow you to improve contrast, increase or decrease brightness, remove noise lines, change the lighting model, flatten the image, among others (Martínez *et al.,* 2016).

According to Avila and Gualteros (2016), these programs allow you to measure the size of the structures of interest captured, build topographic profiles, crop the image to only show the area of interest, zoom in on a particular structure, rotate the image, modify the color palette for illustrative purposes, display the image in 3D, etc. This set of possibilities is of utmost importance to obtain the greatest amount of admissible information from an STM image. Frequently, commercial STM equipment includes some proprietary program for image processing; there are also free programs such as WSxM that can be downloaded from the Internet.

In this sense, Martínez (2022) used a Gwyddion STM image processing program where the different terraces on the surface can be appreciated, applied four filters to a HOPG image with the intention of improving its quality and included a graph that shows a profile drawn perpendicular to the terraces, so that it was possible to observe how the terraces look after applying each filter.

On the other hand, Bohórquez (2017) obtained two emissions that make up the spectrum of the ZnO monocrystal, an intense one centered on 3.2 **eV** corresponding to the bandedge of the semiconductor and another, not common in crystals of high crystalline quality, less intense centered on 2.45 **eV** that corresponds to the emission associated with the presence of oxygen vacancies. which were generated by grain boundaries identified by the STM.

Similarly, Delgado *et al.* (2019), used a Dulcinea model Nanotech control unit and a non-commercial STM, using WSxM software for communication with the system (Horcas *et al.,* 2017) which consists of several commands that allow controlling the microscope, obtaining images of the samples, acquiring data and performing an analysis of them.

Tan and Hang (2019), proposed a magnon field effect transistor that is capable of performing a flow, transmitted and captured by tuning the resonant tunnel through a Dzyaloshinskii-Moriya interaction induced by a gate electric field in the IF intermediate layer. The advantages of such transistors include their wideband frequency width ranging from GHz to THz at room temperature, high scalability, and low intrinsic dissipation with no Joule heat loss.

Calibration of the STM in z

To perform the calibration of the STM in the z-direction, an image of the graphite carbon atoms (HOPG) is used, and knowing the value of their steps, the distances are obtained, from them it is observed what is the necessary calibration factor that must be introduced in the STM so that it is correctly calibrated (Horcas, *et al.,* 2017). In recent studies, Martínez (2022) used values for terraces in HOPG of 0.3354 nm, which is the expected theoretical experimental value for the HOPG steps.

STM Calibration in XY

Calibration in the XY plane is also necessary, for which a HOPG sample is used by comparing the theoretical lattice parameters of the HOPG and the measurements of these parameters in the image taken from the STM. In this way, the correct volt conversion values applied to the piezo system versus distance are adjusted (Horcas, *et al.,* 2017). When comparing the calculated distance (**Lats**) with the measured **distance L**, the latter must obtain a value less than or equal to the calculated distance to determine that the STM is perfectly calibrated in its **XY** (Delgado et al., 2019). For their part, Martínez *et al.* (2016), used atomic resolution images of known surfaces achieving satisfactory results.

Spectroscopy

Spectroscopy in physics refers to the study of the structure of matter, light or their mutual interaction analyzed from an energetic point of view. STM is a powerful technique to study the electronic structure of sample states close to the Fermi energy due to the dependence of the tunneling current on the applied voltage (Bohórquez, 2017).

Tunnel spectroscopy (STS) has two fundamental advantages that make it truly versatile and unique compared to other surface spectroscopy techniques. Firstly, it is a local technique, not averaged over a certain area as is the case with most surface techniques. Spectroscopic information is acquired in real space with atomic resolution, making it possible to study STS of a single atom or molecule isolated on the surface (Vitti *et al.,* 2020).

Likewise, the STM has access to both occupied electronic states and surface voids and therefore it is possible to simultaneously study the valence and conduction bands in the sample; unlike, for example, direct or reverse photoemission where only one of the regions of the electronic spectrum can be accessed (Peña, 2020).

On the other hand, data acquisition for spectroscopy is very similar to topographic data acquisition: on the independent axis you have either the voltage **V** or the spike-sample separation **Z**, while the measurement channel takes data on how the tunnel current varies for a specific point (Delgado *et al.,* 2019). Tunnel spectroscopy is based on the making of curves from which certain information is extracted at a given point on the surface. In this way, from the point of view of electronic transport, it is possible to study, for example, the location of certain states or particular characteristics of the electronic spectrum as well as their spatial extension. There are mainly two types of spectroscopic measurements with spatial resolution, conductance maps and the so-called CITS (Current Imaging Tunneling Spectroscopy) (Peña, 2020).

Therefore, spatially analyzed tunnel spectroscopy is of fundamental importance for the study of the electronic structure of surfaces and nanostructures, as it spatially resolves the local density of sample states (LDOS) at a given energy unlike STM images where the LDOS at each point is the result of the contribution of the electronic states from ***EF*** to ***eV*** (Dakhlaoui *et al.,* 2021).

STM Commercial Equipment

Today, many commercial STM equipment of varying scopes, levels of sophistication, and costs are manufactured. There is also the possibility of manufacturing improvised "homemade" equipment that can be more economical; even so, it is essential to have all the essential components as well as a level of knowledge that allows these components to be properly assembled to produce a functional STM equipment (Horcas *et al.,* 2017).

Among the commercial systems, you can find from simple, compact, economical, easy-to-use and portable devices, to very sophisticated, expensive and high-range devices, whose handling requires in-depth knowledge, skill, and very specific working conditions to exploit all the possibilities they offer.

There are other more sophisticated equipment such as the Omicron VT UHV SPM (manufactured by Omicron Nano Technology), variable temperature (VT) and ultra-high vacuum (UHV), for its acronym in English. It is a high-performance, precision and versatile equipment.

There is also the Park FX40 manufactured by Park Systems, which has an unprecedented mode of control over the distance between the tip and the sample on a sub-nanometer scale. This equipment works automatically, reaches its configuration for probe change and laser alignment, performs the frequency sweep for the cantilever and Z-approach to the sample, the system establishes the necessary parameters for an optimal scan, which it performs continuously until the best images are achieved.

All of this equipment is very expensive and requires very rigorous installation conditions as well as a fairly advanced knowledge of the STM technique, since it requires a lateral resolution of 0.1 nm and 0.01 nm depth resolution, in which the individual atoms are routinely visualized and manipulated (Klapetek and Anderson, 2022).

4. Conclusions

The STM is a very useful instrument in the areas of materials research and other applications of nanotechnology. The implementation of this method presents several challenges of adaptation and implementation in order to achieve optimal performance.

STM can be used in ultra-high vacuum, but it has also been used in water, air, and other ambient liquids or gases, and in temperatures ranging from nearly 0 degrees Kelvin to a few hundred degrees Celsius. The acquisition of reliable topographic images is a direct result of several subsystems that make up the STM.

The STM methodology is a challenging technique as it requires extremely clean and stable surfaces, well-prepared and suitable tips, known calibration samples and excellent vibration and electronic control, the lack of expertise and experience make the process of implementation and functional verification of the system inefficient.

The future of life on the planet will be driven by the application of nanotechnology in equipment and instruments that improve daily activities and solve the problems of an increasingly dynamic society. Nanotechnology has allowed the development of science allowing the obtaining of new materials in the food, pharmaceutical, hydrocarbon, hydrological, and electronic industries, among others.

References

Ávila, J. F., Viatela E., & Gualteros M. M. (2016). Analysis of Electronic Devices of the Tunneling Microscope (STM) for the Design and Simulation of an Optimized Electronic System by SPICE and MATLAB Programming. Francisco José de Caldas District University, Faculty of Engineering, Electronic Engineering Curricular Project. https://repository.udistrital.edu.co/bitstream/handle/11349/3408/AvilaViatelaJairoFernando2016.pdf?sequence=1&isAllowed=y.

Banerjee, S. and P. Zhanga. (2019). A generalized self-consistent model for quantum tunneling current in dissimilar metal-insulator-metal junction. AIP Advances 9, 085302 (2019); doi: 10.1063/1.5116204.

Bohórquez Martínez, C. (2017). Electronic and magnetic properties of ZnO and ZnO films:Mn. Center for Scientific Research and Higher Education of Ensenada, Baja California. https://cicese.repositorioinstitucional.mx/jspui/bitstream/1007/1782/1/tesis_Boh%C3%B3rquez_Mart%C3%ADnez_Carolina_23_nov_2017.pdf.

Dakhlaoui, H., W. Belhadj, and M. B. Wong. (2021). Quantum tunneling mechanisms in monolayer graphene modulated by multiple electrostatic barriers. Results in Physics, Volume 26, 104403. https://doi.org/10.1016/j.rinp.2021.104403.

Delgado-Jiménez, L,. Sabater-Piqueres, C., Chacón-Vargas, S., & Sáenz-Arce, G. (2019). Topographic measurements on atomically flat surfaces under ambient conditions using a tunneling microscope, a didactic approach. UNICIENCIA Vol. 33, No. 1, pp. 30-42. January-June, 2019. DOI: http://dx.doi.org/10.15359/ru.33-1.3.

Field, G. (2022). On the status of quantum tunnelling time. [Preprint] URL: http://philsci-archive.pitt.edu/id/eprint/20829 (accessed 2023-03-06).

Gil-Corrales, J.A.; Vinasco, J.A.; Mora-Ramos, M.E.; Morales A.L. & Duque, C.A. (2022). Study of Electronic and Transport Properties in Double-Barrier Resonant Tunneling Systems. Nanomaterials 12: 1714. https://doi.org/10.3390/nano 12101714.

Goldman, N.; Zepeda-Ruiz, L.; Mullen, R.G.; Lindsey, R.K.; Pham, C.H.; Fried, L.E.; Belof, J.L. (2022). Estimates of Quantum Tunneling Effects for Hydrogen Diffusion in PuO2. Appl. Sci. 12, 11005. doi: https://doi.org/ 10.3390/app122111005.

Hofmann, C., A. S. Landsman and U. Keller. (2019). Attoclock revisited on electron tunneling time. J. Mod. Opt. 66 (10): 1052-1070.

Horcas, I., Fernández, R., Gómez R. J., Colchero, J., Gómez, H. J., & Baro, A. M. (2017). WSXM: A software for scanning probe microscopy and a tol for nanotechnology. Review of Scientific Instruments 78 (013705): 1/9. Doi: http://aip.scitation.org/doi/10.1063/1.2432410. https://www.academia.edu/44975660/Tunnel_Effect.

Ibitola, G. A. and O. Ajanaku. (2016). Quantum Mechanical Potential Step Functions, Barriers, Wells and the Tunneling Effect. World Journal of Applied Physics. Vol. 1, No. 2: 59-66. doi: 10.11648/j.wjap.20160102.15.

Juárez, W. S. & Fernández M. G. (2016) . Symmetries in nature and tunneling: a brief study of double quantum wells. Revista Mexicana de Física E, 62: 86–95.

Juárez, W. S. & G.G. Fernández, M. G. (2018). Symmetries in nature and tunneling: a brief study of double quantum wells. Revista Mexicana de Física E, 62: 86–95.

Klapetek, N. and P. D. Anderson. (2022). Data Levelling and Background Subtraction. gwyddion.net. Retrieved March 17, 2023, from http://gwyddi on.net/documentation/user-guide-en/leveling-and-background.html.

Klimenko, A.Y. (2021). On the effect of decoherence on quantum tunnelling. SN Appl. Sci. 3, 710. https://doi.org/10.1007/s42452-021-04675-5.

Mamedaliev, G. E. (2018). Tunneling microscopy: study of the surface of graphite. http://hdl.handle.net/10810/30530.

Martínez, J. A., J. Valenzuela, M.P. Hernández and J. Herrera. (2016). Automating a scanning tunneling microscope using an OMB-DaqBoard/2000 card and LabVIEW. Revista Mexicana de Física 62 (2016) 45–50.

Martínez, N. (2022). Tunneling microscopy for the study of nanostructures with atomic resolution. University of Cantabria. Faculty of Sciences. https://hdl.handle.net/10902/26376.

Martín-Palma, R. J. (2020). Quantum tunneling in low-dimensional semiconductors mediated by virtual photons. AIP Advances 10: 015145. DOI: 10.1063/1.5133039.

McDonald, C. R., G. Orlando, G. Vampa and T. Brabec. (2015). Tunneling time, what is its meaning?. Journal of Physics: Conference Series 594/012019. DOI:10.1088/1742-6596/594/1/012019.

Moebs, W., S: J. Ling and J. Sanny. (2021). Tunneling of particles through potential barriers. Section URL: https://openstax.org/books/f%C3%ADsica-universitaria-volumen-3/pages/7-6-el-efecto-tunel-de-las-particulas-a-traves-de-las-barreras-de-potencial.

Moreno U. M. (2015). Microscopy and Low-temperature tunneling spectroscopy under UHV conditions: Development of a 4K system and study of the impact of point defects in graphene. Universidad Autónoma de Madrid. Department of Condensed Matter Physics.https://citeseerx.ist.psu.edu/document?repid=rep1&type=pdf&doi=452c3dbb3b9c7eef2e733af5eb13d0bca8f58460.

Oyvind, L. (2020). Quantum tunnelling. DOI: http://book.10.13140/RG.2.2.27225.54883.

Paganini, I. E. and A. E. Pérez. (2011). Tunneling microscopy on graphite and gold surfaces. University of Buenos Aires. Faculty of Exact and Natural Sciences.

Peña, A. (2020). Implementation of lock-in technique in tunneling microscopy under high vacuum conditions. Francisco José de Caldas District University. Faculty of Science and Education. Bachelor's degree in Physics.

Petersen, J. and E. Pollok. (2017). Tunneling flight time, chemistry, and special relativity. J. Phys. Chem. Lett. 8:4017.

Petersen, J. and E. Pollok. (2018). Instantaneous tunneling flight time for wave packet transmission through asymmetric barriers. J. Phys. Chem. A. 122:3563.

Prastowo, S. H., B. Supriadi, Z. R. Ridlo and T. Prihandon. (2020). Tunneling effect on double potential barriers GaAs and PbS. Journal of Physics: Conf. Series1008. DOI:10.1088/1742-6596/1008/1/012020.

Rubio, V. C., Saenz, A. G., Martínez, A. J., Milan, D. C., Moaied, M., Palacios, J. J., Caturla, M. J., & Unitiedt, C. (2017). Grafene flakes obtained by local electroexfoliation of grafite with a STM tip. Physical Chemistry Chemical Physics 19(11): 8061/8068. Doi: http://dx.doi.rg./10.1039/C6CP07236D.

Sainadh, U. S., H. Xu, X. Wang, A. Atía-Tul-Noor, W. C. Wallace, N. Douguet, A. Bray, and V. Litvinyuk. (2019). Attosecond angular streaking and tunneling time in atomic hydrogen. Nature 568: 75-77.

Sanahuja, P. O. (2015). Synthesis and characterization of graphite oxides and graphene hybrids with iron oxides. National University of Distance Education (Spain). http://hdl.handle.net/10261/214601.

Serkovic, L. N. (2009). Study of the surface of Si (111) 7x7 by scanning tunneling microscopy. Pontificia Universidad Católica de Perú. Doi: http://hdl.handle.net/20.00.12404.

Suzuk, A. T., Sales, J. H., & Daykson N. (2020). Quantum tunneling time in the light-front. Proceedings of Science. https://pos.sissa.it/374/091/pdf.

Tang, P. and X. F. Han. (2019). Magnon resonant tunneling effect in double-barrier insulating magnon junctions and magnon field effect transistor. Phys. Rev. B 99, 054401. DOI:https://doi.org/10.1103/PhysRevB.99.054401.

Vitti, J., Mendoza, O., & Marina, S. (2020). Tunneling Microscopy for the Characterization of Nanostructures. Open Institutional Repository. https://doi.org/10.33414/ajea.8.860.2020

Vuković, R. (2021). Talks about quantum tunneling and parallel realities. DOI:

Zhu, Y., X. Yang, F. Yu, R. Wang, Q. Chen, Z. Zhang and Z. Wang. (2022). Quantum tunneling of hydrogen atom transfer affects mandrel degradation in inertial confinement fusion target fabrication. Science 25, 103674. https://doi.org/10.1016/ j.isci.2021.103674.